J. Iron Steel Res. Int.
https://doi.org/10.1007/s42243-018-0089-0

ORIGINAL PAPER

Influences of preparation techniques on glass-forming ability of Fe–P–B–Si–C amorphous alloys

Ji-jun Zhang[1,2,3,4] · Ya-qiang Dong[1,2] · Lu-yang Bie[4] · Qiang Li[4] · Jia-wei Li[1,2] · Xin-min Wang[1,2]

Received: 5 December 2017 / Revised: 2 February 2018 / Accepted: 6 February 2018

Abstract
It has been widely accepted that the ultrafast cooling rate is required for the glass formation of amorphous alloys. Here, the larger glass-forming ability (GFA) of $Fe_{76}P_5(B_{0.5}Si_{0.3}C_{0.2})_{19}$ amorphous alloy was achieved by water quenching at lower cooling rate under argon atmosphere. Cylindrical rods with diameters of 1–2 mm were prepared by water quenching without flux treatment, Cu-mold injection casting, and Cu-mold suction casting, respectively. The influences of the preparation techniques with different cooling rates on GFA, thermal property, and nucleation/growth behavior were examined. The critical diameter of the $Fe_{76}P_5(B_{0.5}Si_{0.3}C_{0.2})_{19}$ amorphous alloys is 1.7 mm for water quenching while smaller than 1.0 mm for injection casting. Microstructure analysis indicates that the crystallization and solidification processes are quite different between the water-quenched and the injection-cast rods. These findings could deepen fundamental understanding on the relationship between the cooling rate, techniques, and GFA of Fe-based amorphous alloys.

Keywords Fe-based amorphous alloy · Preparation technique · Glass-forming ability · Crystallization behavior

1 Introduction

Fe-based amorphous alloys possess considerably superior properties, like good soft magnetic properties, low magnetic loss, high strength, erosion resistance, and low material cost. These unique properties have enabled their application as magnetic functional materials [1–4]. However, the limited glass-forming ability (GFA) of Fe-based amorphous alloys significantly hinders their application in various fields. Thus, it is a long-term objective to develop Fe-based amorphous alloys with three-dimensional size over several millimeters.

To improve the GFA of Fe-based amorphous alloys, intensive efforts have been devoted since the discovery of the first Fe-based bulk metallic glass in 1995 [5]. Generally, for the optimization of GFA, researches are mainly concentrated on two approaches: scavenging heterogeneous nucleation sites in undercooled liquid and improving preparation techniques/conditions. On one hand, methods to scavenge heterogeneous nucleation sites such as using of high-purity materials, flux treatment, rare-earth elements doping, and ultrahigh vacuum casting [6–14] led to improved GFA but increased production cost and cycle time of amorphous alloys. On the other hand, fabrication techniques including rapid quenching, mechanical alloying, and vapor deposition have been applied to supply high-level non-equilibrium conditions in forming Fe-based amorphous alloys [15]. However, it is challenging to increase the cooling rate through the innovation of preparation techniques [16]. Therefore, enhancement of GFA through technique with a moderate cooling rate is the key

✉ Qiang Li
qli@xju.edu.cn

✉ Jia-wei Li
lijw@nimte.ac.cn

1 Key Laboratory of Magnetic Materials and Devices, Ningbo Institute of Materials Technology and Engineering, Chinese Academy of Sciences, Ningbo 315201, Zhejiang, China

2 Zhejiang Province Key Laboratory of Magnetic Materials and Application Technology, Ningbo Institute of Materials Technology and Engineering, Chinese Academy of Sciences, Ningbo 315201, Zhejiang, China

3 University of Chinese Academy of Sciences, Beijing 100049, China

4 School of Physics Science and Technology, Xinjiang University, Urumqi 830046, Xinjiang, China

Published online: 12 June 2018

to the formation and application of Fe-based amorphous alloys.

In recent years, several kinds of Fe-based ferromagnetic amorphous alloys without any glass-forming transition metal elements have been reported [17–21]. Among them, $Fe_{76}P_5(B_{0.5}Si_{0.3}C_{0.2})_{19}$ amorphous alloy fabricated by Cu-mold injection casting under air atmosphere exhibited a critical diameter (d_{cr}) of 3 mm and excellent soft magnetic properties [22]. Here, $Fe_{76}P_5(B_{0.5}Si_{0.3}C_{0.2})_{19}$ amorphous rods were prepared using three different techniques: Cu-mold injection casting, Cu-mold suction casting, and water quenching without flux treatment under argon atmosphere. It is well accepted that the cooling rate of water quenching is much lower than that of injection casting [23, 24]. The d_{cr} of the rod prepared by injection casting was less than 1.0 mm, while the d_{cr} could be improved to 1.0 mm by suction casting and even to 1.7 mm by water quenching. Thus, a dependence of GFA on casting technique was observed for the amorphous alloys. This result indicated that the water quenching technique was beneficial to the glass formation of the present Fe-based alloys, in spite of the low cooling rate and the absence of flux treatment. To investigate the mechanism of this counterintuitive phenomenon, structure characterization was performed on the partially amorphous rods and crystallization behavior during solidification was analyzed. This paper aims to present the experimental evidences for the higher GFA of Fe–Si–B–P–C alloys prepared by water quenching at lower cooling rate and explore the reason for the improvement in GFA.

2 Materials and experimental methods

A multicomponent alloy ingot with nominal atomic composition of $Fe_{76}P_5(B_{0.5}Si_{0.3}C_{0.2})_{19}$ was prepared by induction melting the mixtures of pure Fe (99.99 mass%), B (99.9 mass%), and Si (99.999 mass%), pre-alloyed Fe_3P (99.99 mass%, 18 mass% P), and Fe–C (99.99 mass%, 3.6 mass% C) alloys under high purity of argon atmosphere.

Cylindrical rods with diameters of 1.0 and 1.5 mm were prepared by injection casting and suction casting techniques, respectively. Their cooling rates were estimated to be $\sim$ 4000 K/s [24]. In addition, rods of 1.5–2.0 mm in diameters and a few centimeters in length were prepared by water quenching, without flux treatment, at a cooling rate of $\sim$ 100 K/s [23]. The details of water quenching process used in the present study were described elsewhere [21, 25]. $Fe_{76}P_5(B_{0.5}Si_{0.3}C_{0.2})_{19}$ amorphous ribbons with a thickness of 25 μm were also prepared for comparison by the melt spinning method.

Amorphous nature of the as-cast alloys was ascertained using an X-ray diffractometer (XRD) with Cu Kα radiation. Thermal behavior was examined by differential scanning calorimetry (DSC) at a heating rate of 40 K/min. Microstructure on the longitudinal cross section of the rods was investigated using an optical microscope (OM) and a scanning electron microscope (SEM). The chemical composition of the crystallites was estimated with an energy-dispersive X-ray spectroscope (EDX). All the measurements were conducted at room temperature.

3 Results and discussion

Figure 1a gives the sticks in diameter of 1.5–2.0 mm prepared by water quenching. Figure 1b shows the XRD patterns of $Fe_{76}P_5(B_{0.5}Si_{0.3}C_{0.2})_{19}$ rods prepared by injection casting, suction casting, and water quenching techniques in argon atmosphere. The patterns of the rods fabricated using injection casting (ϕ1.0 mm) and suction casting (ϕ1.5 mm) exhibit crystalline diffraction peaks identified as α-Fe and $Fe_3(B,P,C)$ phases, suggesting that the rods cast at higher cooling rates are with partially amorphous structure. In contrast, the specimen can be cast into fully amorphous rods with diameters to 1.0 mm for suction casting and up to 1.7 mm for water quenching, as

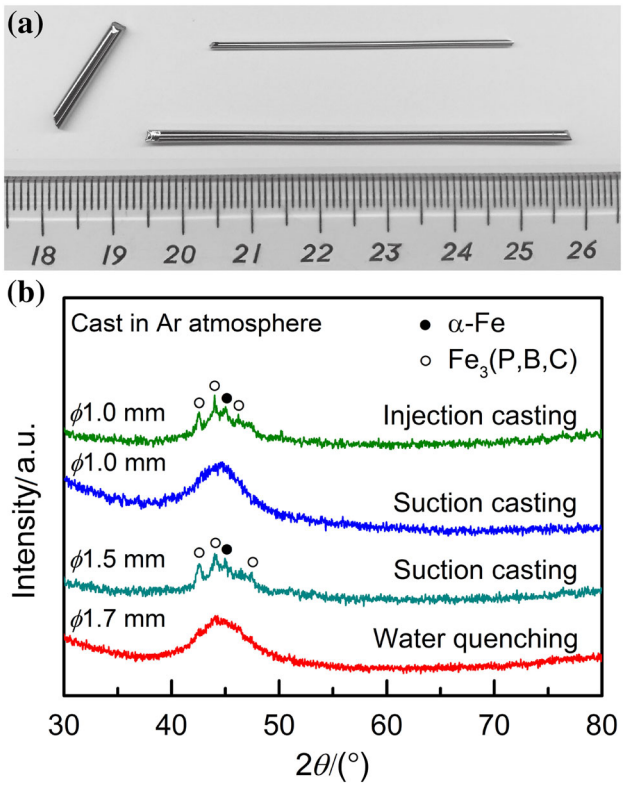

Fig. 1 Photograph of amorphous rods in diameter of 1.5–2.0 mm prepared by water quenching technique (**a**) and XRD patterns of $Fe_{76}P_5(B_{0.5}Si_{0.3}C_{0.2})_{19}$ amorphous rods and partially amorphous rods produced by different techniques in argon atmosphere (**b**)

only a broad halo peak without any apparent crystalline peaks is observed. Namely, the d_{cr} of $Fe_{76}P_5(B_{0.5}Si_{0.3}C_{0.2})_{19}$ amorphous alloy increases from less than 1.0–1.7 mm by replacing injection casting with water quenching as the fabrication technique, which reveals that the water quenching technique with lower cooling rate is more favorable for the formation of Fe–Si–B–P–C amorphous alloys than injection casting and suction casting techniques.

Figure 2 shows the DSC traces of the $Fe_{76}P_5(B_{0.5}Si_{0.3}C_{0.2})_{19}$ rods prepared by different techniques, together with that for the melt-spun ribbon. Apparent glass transitions and sharp crystallization peaks are observed in the ribbon and the entirely amorphous rods prepared by suction casting (ϕ1.0 mm) and water quenching (ϕ1.7 mm), confirming the amorphous nature of the rods. The Curie temperature (T_c), glass transition temperature (T_g), and onset of crystallization temperature (T_x) of the water-quenched rod shift slightly to higher temperature compared with that of the melt-spun ribbon. The gradually increased glass transition temperature of the samples may be due to the decrease in cooling rates of the solidification process [26]. The water-quenched amorphous rod may have a much denser atomic packing and a more relaxed atomic configuration than the more quickly solidified counterpart [27]. The increase in crystallization temperature is thought to be caused by the decrease in surface as samples size rises; according to Liu et al. [26], the larger surface tended to provide more nucleation sites for crystallization. Besides, the varying degree of structural relaxations generated during solidification process gave rise to the variation of physical and thermal properties [28]. Liebermann et al. [29] showed that T_c was sensitive to the degree of relaxation, rising when the as-prepared amorphous alloy was annealed. Thus, the increase in T_c also verifies a more relaxed amorphous structure in water-quenched rod.

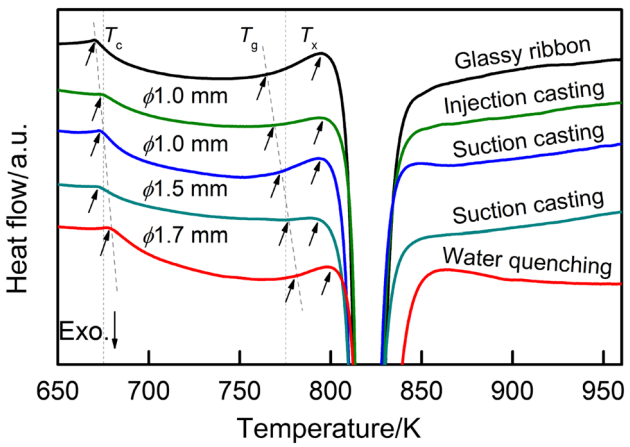

Fig. 2 DSC traces of $Fe_{76}P_5(B_{0.5}Si_{0.3}C_{0.2})_{19}$ melt-spun ribbon and bulk samples prepared by injection casting (ϕ1.0 mm), suction casting (ϕ1.0 and ϕ1.5 mm), and water quenching (ϕ1.7 mm) in argon atmosphere at a heating rate of 40 K/min

Microstructure analysis demonstrates a significant difference between the partially amorphous $Fe_{76}P_5(B_{0.5}Si_{0.3}C_{0.2})_{19}$ rods manufactured by injection casting and water quenching methods (Fig. 3). OM observations were performed on the longitudinal section of the rods with diameters just above the d_{cr}, namely rods with diameters of 1.0 mm for injection casting, 2.0 mm for water quenching, and 1.5 mm for suction casting (Fig. 3a–c). Injection-cast rod (ϕ1.0 mm) exhibits a series of large grains with diameter of 50–100 μm present in the center region and oriented parallel to the longitudinal direction (Fig. 3a). Figure 3b shows that a high number density of the 10–20 μm spherical grains is embedded uniformly in the amorphous matrix, and reveals an amorphous/crystalline dual-phase structure in water-quenched Fe-based rod of 2.0 mm in diameter. This is consistent with the concept that the nuclei formed at a maximum nucleation rate tended to experience a much lower growth rate [15]. Similarly, suction-cast rod (ϕ1.5 mm) displays a structure comprising crystalline phases in diameter of 20–40 μm dispersed in amorphous matrix. As a result, the water-quenched rod possesses a homogeneous structure, making it totally different from the center-crystallized structure of injection-cast rod. This implies that the crystallization behavior is controlled by nucleation in injection casting process, but it is particle growth dominated in water quenching process.

The crystalline structures of the partially amorphous samples were further investigated by SEM (Fig. 3d–f). Injection-cast rod (Fig. 3d) exhibits large ($\sim$ 60 μm) dendrite grains grown from inside-out, with secondary dendrites present along the primary dendrites. This is similar to the columnar growth of dendrite in aluminum alloys and was controlled by the high and directional heat flux in the additive manufacture process, which supplies high thermal gradients and small undercooling during solidification [30]. In contrast, fine microstructures are acquired via water quenching process by suppressing the growth of secondary dendrites (Fig. 3e). The fine and diffusely distributed grains are thought to form in identical solidification conditions, which arise from the inferior thermal conductivity of quartz glass. In conclusion, the crystallization during solidification is controlled by nucleation mechanism for injection casting, whereas by grain growth mechanism for water quenching. The elemental compositions of the grains were evaluated with the EDX resulted from SEM analysis (Table 1). The EDX analysis reveals that the ratio of Fe:P:Si in all amorphous matrix is approximately 76:5:4.7, which is similar to the nominal composition $Fe_{76}P_5(B_{0.5}Si_{0.3}C_{0.2})_{19}$. The EDX signals from B and C elements are high in intensity and far deviate from the nominal composition, because B and C elements are

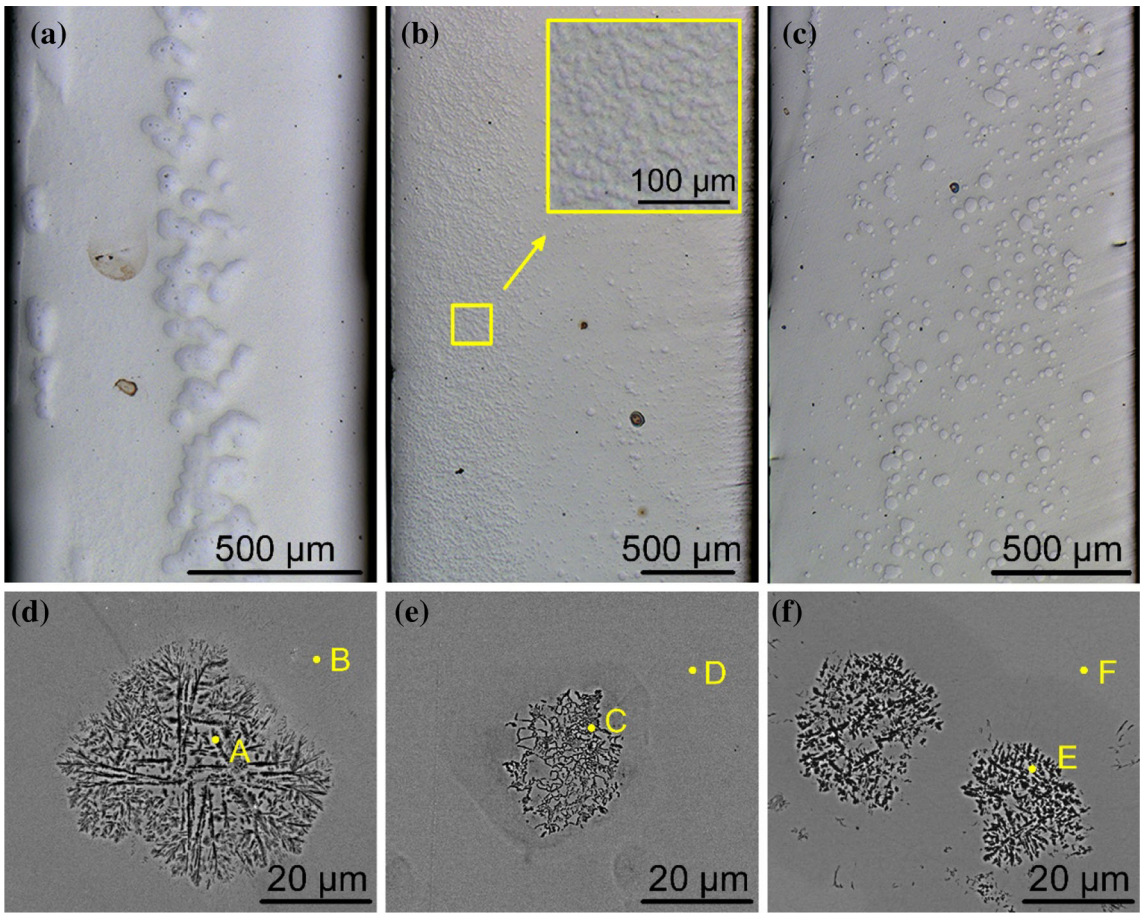

Fig. 3 Optical micrograph (**a**, **b**, **c**) and SEM images (**d**, **e**, **f**) in longitudinal section of partially amorphous $Fe_{76}P_5(B_{0.5}Si_{0.3}C_{0.2})_{19}$ rods produced by injection casting with a diameter of 1.0 mm (**a**, **d**), water quenching with a diameter of 2.0 mm (**b**, **e**) and suction casting with a diameter of 1.5 mm (**c**, **f**). The inset shows enlarged view of the square region in (**b**)

Table 1 Compositions of partially amorphous $Fe_{76}P_5(B_{0.5}Si_{0.3}C_{0.2})_{19}$ alloys prepared by different techniques, estimated from EDX analysis (at.%)

Method	Point	Fe	P	B	Si	C	O
Injection casting	A	24.01	2.69	20.38	1.58	39.72	11.62
	B	34.97	2.44	25.89	2.60	32.22	1.88
Water quenching	C	38.06	2.55	18.23	2.58	29.14	9.44
	D	32.88	2.28	21.71	2.41	38.26	2.46
Suction casting	E	29.43	1.95	21.09	2.11	35.06	10.36
	F	27.59	1.98	29.52	1.84	36.23	2.83

not detectable by EDX. Surprisingly, the oxygen content of the grains, irrespective of their size and morphology, are several times that of the amorphous matrix, such as six times the injection-cast samples while less than four times the others. This phenomenon suggests that proper oxygen content can enhance the GFA of the present Fe-based amorphous alloys, which is also reported in other Fe-based amorphous alloys [31, 32].

Here, reasons are proposed to be responsible for this abnormal phenomenon. First, the inert quartz tube with low thermal conductivity employed in water quenching plays an important role in preparation of Fe-based amorphous alloy [25]. For water quenching process, a humble temperature gradient results in microstructure with grain size of about 10–20 μm, five times smaller than the grains formed in injection casting at a steep temperature gradient. Recently, flexible materials for electromagnetic shielding

with aligned and isotropic porous structures were designed by tuning the temperature gradient in freezing process [33].

Second, nucleation during solidification needs two requirements, energetically favorable condition and nucleation sites [30]. In the water quenching process, the molten alloy in quartz tube was first placed in a furnace at 1450 K for 300 s, and then quenched in salted ice-water. The high-temperature isothermal treatment allows for a more homogeneous and stable melt that prevents heterogeneous nucleation in the following solidification process [25]. In the case of the injection casting process, the molten alloy was immediately injected into Cu-mold cavity, solidifying quickly and turbulently. During ejection, the melt in contact with the Cu-mold was rapidly cooled below the liquidus temperature, forming a steep temperature gradient from inside-out. When the high-speed ejected melt stroke at the bottom of the Cu-mold, it rolled up due to the eddy effects caused by the limited space in Cu-mold [15]. As a result, stirring of molten alloy accelerates the heterogeneous nucleation and the high temperature in the inner region provides an energetically favorable condition to grains growth. In order to verify this, rod with diameter of 1.5 mm was cast into a Cu-mold by suction casting, showing similar cooling rate as injection casting. The previous research has proved that suction casting could suppress the heterogeneous nucleation and casting defects such as cavity and holes during solidification [31]. The substantial differences presented in grain size, morphology, density, and distribution confirm that the injection-cast liquid is more desired to crystallize during cooling.

The different crystallization and solidification behaviors between the injection casting and the water quenching techniques are also related to the dynamic process. The transformation rates of liquid-crystal are generally dominated by the density of nucleation and the diffusion of the atoms. According to Porter and Esterling [34], the nucleation rate (I_s), which describes the stability of undercooled liquid, can be expressed as:

$$I_s = D \cdot \exp\left[-\frac{A \cdot S(\theta)}{(\Delta T)^2}\right] \quad (1)$$

where D is the atomic diffusion coefficient; ΔT is the crystallization undercooling; A is a constant which is insensitive to temperature; and $S(\theta)$ is the shape factor. According to Inoue [35], hindering atomic diffusivity during the cooling process could depress the nucleation rates, increase the undercooling, and improve the GFA. Concerning the humble temperature gradient, homogeneous liquid phase, and the diffusely distributed grains, the water quenching technique is supposed to have a larger undercooling and reach the degree of maximum nucleation rate.

From the melt state side, the solidification process can be deemed as: (A) liquid splash/impact quenching for the injection casting, (B) massive stream liquid quenching for the suction casting, and (C) silent water quenching. The results indicate substantial difference in the equilibrium liquidus temperature and undercooled condition of these three processes [30]. Figure 4 depicts a nose-shaped continuous-cooling-transformation (CCT) diagram to predict the crystallization and solidification behaviors. The cooling rates of the Fe-based rods reduce from injection casting (1.0 mm) to suction casting (1.5 mm), and to water quenching (1.7 mm). The heterogeneous nucleation temperature is the highest for the injection casting, followed by the suction casting and then the water quenching. That is, for injection casting, the nose points of the CCT curve lies in short time and high-temperature side, in which region the crystallization mechanism is growth governed [36]. While for water quenching, the nose points shift to longer time and lower temperature, where the crystallization process is dominated by nucleation [37]. The nose point for the suction casting is placed in the medium range. It has also documented that the maximum nucleation always appeared at a lower temperature than the maximum growth of the grains [38]. As a result, in injection casting, the turbulent melt and high thermal gradient make it less stable and more desire to crystallize and grow up, while for water quenching, the large undercooling inhibits the heterogeneous nucleation and depresses the dendritic growth.

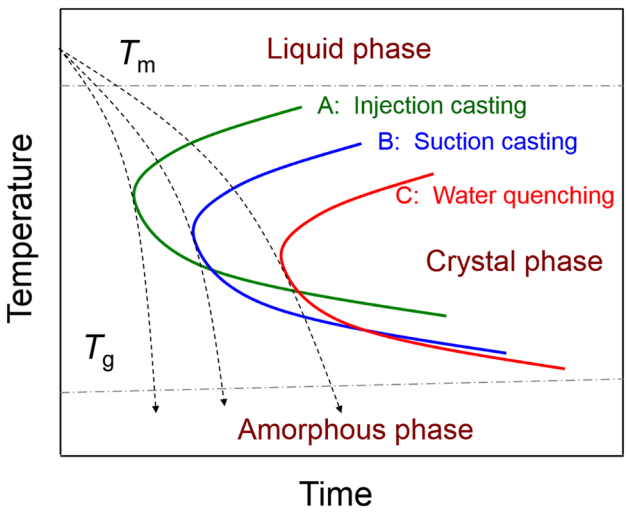

Fig. 4 Schematic continuous–cooling–transformation (CCT) diagram for $Fe_{76}P_5$ $(B_{0.5}Si_{0.3}C_{0.2})_{19}$ amorphous alloys prepared by injection casting (**A**), suction casting (**B**), and water quenching processes (**C**)

4 Conclusions

1. $Fe_{76}P_5(B_{0.5}Si_{0.3}C_{0.2})_{19}$ amorphous alloys with diameter of $\sim$ 1.7 and 1.0 mm are prepared in argon atmosphere by water quenching and suction casting technique, respectively. For injection casting, the glass-forming ability is less than 1.0 mm.
2. The improvement in the glass-forming ability in water quenching method is owing to the homogenous and silent cooling of the molten alloy placed in the inert quartz tube. The high-temperature isothermal treatment and humble temperature gradient lead to a more stable and homogeneous liquid phase, thus suppressing the heterogeneous nucleation and crystalline growth.
3. This work provides a fundamental understanding on the relationship among the cooling rates, preparation techniques, and glass-forming ability of Fe-based amorphous alloys. The proper adjustment of the water quenching and suction casting techniques is expected to contribute to a further improvement in GFA of Fe-based amorphous alloys.

Acknowledgements This work was supported by the National Key Research and Development Program of China (Grant No. 2016YFB0300500), National Natural Science Foundation of China (Grant Nos. 51561028 and 51771161), and Ningbo Municipal Natural Science Foundation (Grant No. 2017A610034).

References

[1] M.J. Duarte, J. Klemm, S.O. Klemm, K.J.J. Mayrhofer, M. Stratmann, S. Borodin, A.H. Romero, M. Madinehei, D. Crespo, J. Serrano, S.S.A. Gerstl, P.P. Choi, D. Raabe, F.U. Renner, Science 341 (2013) 372–376.
[2] C. Suryanarayana, A. Inoue, Int. Mater. Rev. 58 (2013) 131–166.
[3] W.M. Yang, H.S. Liu, Y.C. Zhao, A. Inoue, K.M. Jiang, J.T. Huo, H.B. Ling, Q. Li, B.L. Shen, Sci. Rep. 4 (2014) 6233.
[4] F. Wang, A. Inoue, Y. Han, S.L. Zhu, F.L. Kong, E. Zanaeva, G.D. Liu, E. Shalaan, F. Al-Marzouki, A. Obaid, J. Alloy. Compd. 723 (2017) 376–384.
[5] T.D. Shen, R.B. Schwarz, Appl. Phys. Lett. 75 (1999) 49–51.
[6] W.H. Wang, Prog. Mater. Sci. 52 (2007) 540–596.
[7] A. Chrobak, V. Nosenko, G. Haneczok, L. Boichyshyn, B. Kotur, A. Bajorek, O. Zivotsky, A. Hendrych, Mater. Chem. Phys. 130 (2011) 603–608.
[8] W.H. Wang, M.X. Pan, D.Q. Zhao, Y. Hu, H.Y. Bai, J. Phys.: Condens. Matter 16 (2004) 3719–3723.
[9] V. Ponnambalam, S.J. Poon, G.J. Shiflet, J. Mater. Res. 19 (2004) 3046–3052.
[10] H. Jian, W. Luo, S. Tao, M. Yan, J. Alloy. Compd. 505 (2010) 315–318.
[11] S.L. Lin, S.F. Chen, J.K. Chen, Y.L. Lin, Intermetallics 18 (2010) 1826–1828.
[12] T. Bitoh, A. Makino, A. Inoue, A.L. Greer, Appl. Phys. Lett. 88 (2006) 182510.
[13] Z.P. Lu, C.T. Liu, J.R. Thompson, W.D. Porter, Phys. Rev. Lett. 92 (2004) 245503.
[14] Z.P. Lu, C.T. Liu, W.D. Porter, Appl. Phys. Lett. 83 (2003) 2581–2583.
[15] J. Schroers, Adv. Mater. 22 (2010) 1566–1597.
[16] W.L. Johnson, G. Kaltenboeck, M.D. Demetriou, J.P. Schramm, X. Liu, K. Samwer, C.P. Kim, D.C. Hofmann, Science 332 (2011) 828–833.
[17] B.L. Shen, M. Akiba, A. Inoue, Appl. Phys. Lett. 88 (2006) 131907.
[18] Z.B. Jiao, H.X. Li, Y. Wu, J.E. Gao, S.L. Wang, S.H. Yi, Z.P. Li, Sci. China, Ser. G 53 (2010) 430–434.
[19] J. Wang, R. Li, N. Hua, L. Huang, T. Zhang, Scripta Mater. 65 (2011) 536–539.
[20] A. Makino, T. Kubota, C.T. Chang, M. Makabe, A. Inoue, Mater. Trans. 48 (2007) 3024–3027.
[21] Q. Li, J. Li, P. Gong, K. Yao, J. Gao, H. Li, Intermetallics 26 (2012) 62–65.
[22] A. Makino, C.T. Chang, T. Kubota, A. Inoue, J. Alloy. Comp. 483 (2009) 616–619.
[23] Q. Li, Metall. Mater. Trans. B 40 (2009) 405–410.
[24] X.H. Lin, W.L. Johnson, J. Appl. Phys. 78 (1995) 6514–6519.
[25] Q. Li, Mater. Lett. 60 (2006) 3113–3117.
[26] Y.H. Liu, D. Wang, K. Nakajima, W. Zhang, A. Hirata, T. Nishi, A. Inoue, M.W. Chen, Phys. Rev. Lett. 106 (2011) 125504.
[27] Y.Q. Cheng, E. Ma, Prog. Mater. Sci. 56 (2011) 379–473.
[28] X. Hu, S.C. Ng, Y.P. Feng, Y. Li, Phys. Rev. B 64 (2001) 172201.
[29] H. Liebermann, C. Graham, P. Flanders, IEEE Trans. Magn. 13 (1977) 1541–1543.
[30] J.H. Martin, B.D. Yahata, J.M. Hundley, J.A. Mayer, T.A. Schaedler, T.M. Pollock, Nature 549 (2017) 365–369.
[31] C.T. Chang, J.H. Zhang, B.L. Shen, W.H. Wang, A. Inoue, J. Mater. Res. 29 (2014) 1217–1222.
[32] H.X. Li, J.E. Gao, Z.B. Jiao, Y. Wu, Z.P. Lu, Appl. Phys. Lett. 95 (2009) 161905.
[33] Z.H. Zeng, H. Jin, M.J. Chen, W.W. Li, L.C. Zhou, X. Xue, Z. Zhang, Small 13 (2017) 1701388.
[34] D.A. Porter, K.E. Esterling, Phase transformations in metals and alloys, 2nd ed., CRC Press, Boca Raton, 1992.
[35] A. Inoue, Mater. Trans. JIM 36 (1995) 866–875.
[36] J. Schroers, Y. Wu, R. Busch, W.L. Johnson, Acta Mater. 49 (2001) 2773–2781.
[37] J. Schroers, W.L. Johnson, R. Busch, Appl. Phys. Lett. 76(2000) 2343–2345.
[38] J. Schroers, A. Masuhr, W.L. Johnson, R. Busch, Phys. Rev. B 60 (1999) 11855.